iScience

CellPress
OPEN ACCESS

Article

Y chromosome damage underlies testicular abnormalities in ATR-X syndrome

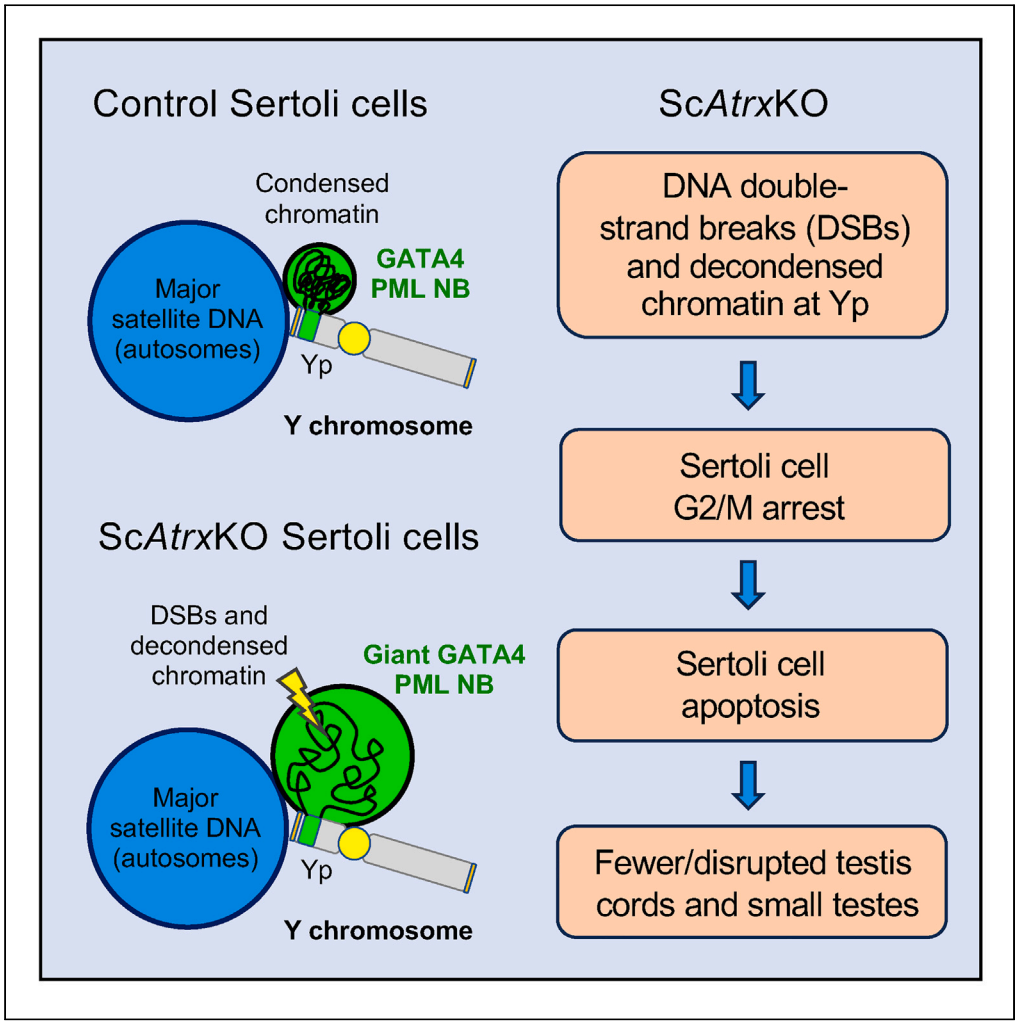

Nayla Y. León, Thanh Nha Uyen Le, Andrew Garvie, Lee H. Wong, Stefan Bagheri-Fam, Vincent R. Harley

vincent.harley@hudson.org.au

Highlights

Mouse Sertoli cells contain a novel GATA4-positive PML NB at chromosome Yp

ATRX loss leads to DNA damage and chromosome condensation failure at the Yp PML NB

The Yp defects lead to Sertoli cell G2/M arrest and death and small testes in mice

Yp damage is a novel mechanism for the testicular defects in ATR-X syndrome

León et al., iScience 27, 109629
May 17, 2024 © 2024 Published by Elsevier Inc.
https://doi.org/10.1016/j.isci.2024.109629

iScience

CellPress
OPEN ACCESS

Article

Y chromosome damage underlies testicular abnormalities in ATR-X syndrome

Nayla Y. León,[1,2] Thanh Nha Uyen Le,[1,2] Andrew Garvie,[3] Lee H. Wong,[3] Stefan Bagheri-Fam,[1,2] and Vincent R. Harley[1,2,4,*]

SUMMARY

ATR-X (alpha thalassemia, mental retardation, X-linked) syndrome features genital and testicular abnormalities including atypical genitalia and small testes with few seminiferous tubules. Our mouse model recapitulated the testicular defects when *Atrx* was deleted in Sertoli cells (Sc*Atrx*KO) which displayed G2/M arrest and apoptosis. Here, we investigated the mechanisms underlying these defects. In control mice, Sertoli cells contain a single novel "GATA4 PML nuclear body (NB)" that contained the transcription factor GATA4, ATRX, DAXX, HP1α, and PH3 and co-localized with the Y chromosome short arm (Yp). Sc*Atrx*KO mice contain single giant GATA4 PML-NBs with frequent DNA double-strand breaks (DSBs) in G2/M-arrested apoptotic Sertoli cells. HP1α and PH3 were absent from giant GATA4 PML-NBs indicating a failure in heterochromatin formation and chromosome condensation. Our data suggest that ATRX protects a Yp region from DNA damage, thereby preventing Sertoli cell death. We discuss Y chromosome damage/decondensation as a mechanism for testicular failure.

INTRODUCTION

ATRX (alpha thalassemia, mental retardation, X-linked) is a chromatin remodeling protein which belongs to the switch/sucrose non-fermentable (SWI-SNF) family. Mutations in *ATRX* cause the ATR-X syndrome, characterized by distinct craniofacial features, severe intellectual disability, alpha thalassemia, and urogenital abnormalities.[1–4] ATRX protein has multiple important biological functions such as in the formation and maintenance of pericentromeric and telomeric heterochromatin, chromosome condensation, and in the protection of common fragile sites, pericentromeric heterochromatin, and telomeres during replication.[5] ATRX can recruit heterochromatin protein 1 alpha (HP1α) at pericentromeric heterochromatin.[6] Within promyelocytic leukemia nuclear bodies (PML NBs) ATRX and its interacting partner death domain associated protein (DAXX) deposit the histone variant H3.3 at pericentromeric heterochromatin and telomeres.[7–11] During replication, ATRX and DAXX facilitate replication by preventing G4 quarter DNA structure formation and also promote replication fork recovery and homologous recombination-dependent repair of DNA double-strand breaks (DSBs).[5,8,12–16]

PML NBs are sub-nuclear structures involved in various cellular functions such as replication, gene regulation, apoptosis, heterochromatin condensation, telomere integrity, and DNA damage response.[17–23] They are extensively distributed, being found in most cell lines and many tissues. The number of PML NBs varies from 5 to 30 per nucleus. Under normal conditions, PML NBs size ranges from 0.1 to 1.0 μm in diameter.[24,25] The protein components of the inner core are highly variable. To date, over 250 different proteins have been described to be recruited by PML NBs including ATRX and DAXX.[26–28] Recently, the short arm of the Y chromosome (Yp) has been identified as a region to which PML NBs frequently bind.[29] No function of PML NBs during sex development or in differences/disorders of sex development (DSD) has been demonstrated to date.

A common feature in ATR-X syndrome is an atypical sex development affecting XY individuals. Patients display genital abnormalities varying in severity from cryptorchidism to complete female external genitalia. Gonadal histology reveals small testes containing only a few seminiferous tubules.[2,30] Previously we generated an *Atrx* knockout mouse model with *Atrx* specifically inactivated in Sertoli cells (Sc*Atrx*KO), a cell lineage crucial for formation of testis cords, the presumptive seminiferous tubules. Like boys with ATR-X syndrome, Sc*Atrx*KO mice showed small testes with fewer tubules. The lack of tubules was due to G2/M cell-cycle arrest and apoptosis of Sertoli cells during fetal life.[31]

In this study, we describe a single novel PML nuclear body we call "GATA4 PML-NB" in testicular Sertoli cells that encapsulates the short arm of the Y chromosome and expresses the transcription factor GATA4 in a novel structural role. The GATA4 PML-NB contains ATRX, DAXX, and HP1α and shows early enrichment of phospho-histone H3 (PH3), a marker of chromosome condensation at G2. In Sc*Atrx*KO mice, these GATA4 PML-NBs are enlarged and are associated with DNA double-stranded breaks in G2/M-arrested Sertoli cells that undergo apoptosis.

[1]Hudson Institute of Medical Research, Melbourne, VIC 3168, Australia
[2]Department of Molecular & Translational Science, Monash University, Melbourne, VIC 3168, Australia
[3]Department of Biochemistry and Molecular Biology, Biomedicine Discovery Institute, Monash University, Wellington Road, Clayton, VIC 3800, Australia
[4]Lead contact
*Correspondence: vincent.harley@hudson.org.au
https://doi.org/10.1016/j.isci.2024.109629

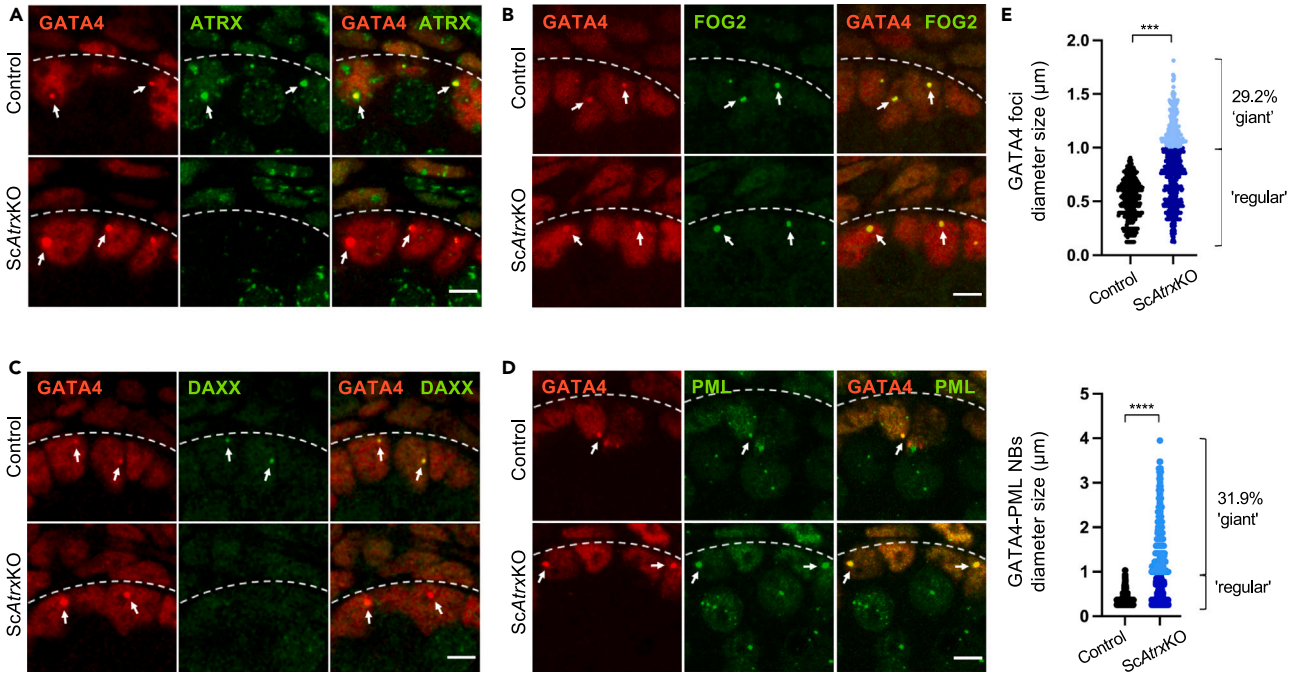

Figure 1. Sertoli cells contain a novel GATA4 PML-NB which is enlarged in the absence of ATRX

(A–D) Double immunofluorescence (IF) analyses in E16.5 XY control and Sc*Atrx*KO testes. Dashed lines mark the basal lamina of the testis cords. White arrows denote GATA4 foci. At least 100 GATA4 foci were analyzed per testis ($n = 3$). Scale bars represent 5 µm. (A) Double IF for GATA4 (red, nuclear) and ATRX (green, nuclear). (B) Double IF for GATA4 (red, nuclear) and FOG2 (green, nuclear). (C) Double IF for GATA4 (red, nuclear) and DAXX (green, nuclear). (D) Double IF for GATA4 (red, nuclear) and PML (green, nuclear).

(E) Measurements of GATA4 foci and GATA4-PML NB diameters. More than 100 GATA4 foci and GATA4-PML NBs were measured in each testis (control, $n = 3$; Sc*Atrx*KO, $n = 4$), using Fiji software.[32] The control is represented in black and the Sc*Atrx*KO in blue. Dark blue shows GATA4 foci and GATA4-PML NBs that have a regular size in Sc*Atrx*KO Sertoli cells, while light blue shows GATA4 foci and GATA4-PML NBs outside the control range. ***$p < 0.001$, ****$p < 0.0001$; unpaired two-tailed t test compared to control.

See also Figure S1.

The absence of HP1α and PH3 at the GATA4 foci in giant PML NBs indicates a defect in heterochromatin formation and chromosome condensation, respectively. Our results suggest Y chromosome damage as a novel mechanism in the etiology of ATR-X syndrome.

RESULTS

A single novel PML NB is enlarged in *Atrx* knockout Sertoli cells

Conditional knockout of *Atrx* in the Sertoli cells of the fetal mouse testis (Sc*Atrx*KO) leads to cell-cycle arrest at G2/M and associated apoptosis.[31] With further investigation, we observed an unusual staining pattern of GATA4 in Sertoli cells of both control and Sc*Atrx*KO gonads (Figure 1A). GATA4 is important for testis development and reportedly shows diffuse expression throughout the nucleus.[33,34] In addition to this diffuse expression, we found that around 10% of control and 26% of Sc*Atrx*KO Sertoli cells contain a single GATA4 immunoreactive nuclear speckle (GATA4 foci), frequently located near the periphery of the nucleus (Figure 1A; Table 1). Some GATA4 foci were significantly larger in Sc*Atrx*KO when compared to control testes; the size range in the control testes was 0.1–1 µm, whereas in the Sc*Atrx*KO, it was 0.2–2 µm, with around 29% of Sertoli cells containing enlarged (giant) GATA4 foci outside of the control range (>1.0 µm; Figure 1E).

To investigate if these giant GATA4 foci could be a direct consequence of ATRX loss at these sites, we performed co-immunofluorescence (co-IF) for GATA4 and ATRX (Figures 1A and S1). As expected, ATRX showed diffuse nuclear expression and moderate levels at the bright DAPI regions (chromocenters) that contain the highly compacted pericentromeric heterochromatin (major satellites) of the chromosomes.[35] Sertoli cells also showed a single nuclear speckle with strong ATRX IF staining intensity that co-localized with the GATA4 foci, located near one of the bright DAPI regions (Figures 1A and S1). This suggests that ATRX has an important function at these foci. We next looked for the presence of two well-studied interacting partners of GATA4 and of ATRX at the GATA4 foci, FOG2 and DAXX, respectively. Co-IF for GATA4 and FOG2 revealed co-localization in both control and Sc*Atrx*KO Sertoli cells (Figure 1B). While DAXX co-localized with the GATA4 foci in control gonads, it was absent in Sc*Atrx*KO Sertoli cells (Figure 1C), indicating that presence of DAXX depends on ATRX.

ATRX and DAXX are well-known components of PML NBs.[26–28] We investigated whether GATA4 foci might associate with PML NBs. Co-IF for GATA4 and PML in control Sertoli cells revealed that 17% of GATA4 foci co-localized with one specific PML NB, whereas the other 83%

Table 1. Percentage of Sertoli cells with single GATA4 foci in control and Sc*Atrx*KO testes

	Control	KO
Animals	*n* = 3	*n* = 3
Number of Sertoli cells	1145	962
Sertoli cells with single GATA4 foci	119	251
Percentage: Sertoli cells with single GATA4 foci	**10.4%**	**26.1%**

were PML-negative (Figure 1D; Table 2). In contrast, in Sc*Atrx*KO testes, 77% of the regular sized GATA4 foci (upto 1.0 μm) co-localized with the PML NBs and almost all (94%) of the giant GATA4 foci (>1.0 μm) were positive for PML. Around 32% of GATA4 PML-NBs in Sc*Atrx*KO Sertoli cells were larger than the control range (Figure 1E). Therefore, the giant GATA4 foci are the giant PML NBs in the Sc*Atrx*KO Sertoli cells. Taken together, these data suggest that PML is recruited to the ATRX-GATA4 foci in both control and Sc*Atrx*KO Sertoli cells, but to far a greater extent in Sc*Atrx*KO Sertoli cells.

Sc*Atrx*KO Sertoli cells with giant GATA4 PML-NBs are arrested at G2/M

The G2/M phase of the cell cycle is prolonged in Sertoli cells of Sc*Atrx*KO mice when compared to control mice.[31] However, the underlying mechanism remained elusive. We examined if the giant GATA4 foci in Sc*Atrx*KO Sertoli cells are related to the cell-cycle defect, by co-IF for GATA4 and PH3, a cell cycle marker of late G2 and M phase.[36] PH3 IF staining confirmed that Sc*Atrx*KO testes have more Sertoli cells at G2/M than control testes (23.5% versus 14.6%) (Figures 2A and 2B). When considering only those Sertoli cells with GATA4 foci, control testes have more GATA4 foci positive Sertoli cells at G2/M (49.6%) (Figure 2C) when compared to the entire Sertoli cell population (14.6%) (Figure 2B). Similarly, the percentage of Sc*Atrx*KO Sertoli cells with regular sized GATA4 foci at G2/M (44.6%) (Figure 2C) was higher than in the entire Sertoli cell population (23.5%) (Figure 2B). Strikingly, Sc*Atrx*KO Sertoli cells with giant GATA4 foci were all at G2/M, showing strong speckled PH3 staining typical of cells at late G2 phase (Figures 2A and 2C).[36]

These data show that Sertoli cells with GATA4 foci in both control and Sc*Atrx*KO testes are enriched at late G2/M phase. Furthermore, all Sc*Atrx*KO Sertoli cells with giant GATA4 foci are arrested at G2/M. Therefore, it is likely that a defect at the enlarged GATA4 foci underlies the G2/M cell-cycle arrest in Sc*Atrx*KO Sertoli cells.

Loss of ATRX at the GATA4 foci leads to DNA DSBs and Sertoli cell apoptosis

ATRX reportedly protects common fragile sites, pericentromeric heterochromatin, and telomeres prone to DNA DSBs under conditions of replication stress.[12–16] DSBs trigger the cell to activate the DNA damage response to repair DNA.[37] One of the earliest and important chromatin changes during this process is the phosphorylation of the histone variant H2AX (γ-H2AX) around the DSB sites.[38] γ-H2AX recruits DNA repair proteins and induces G2/M cell-cycle arrest which will result in either DNA repair or apoptosis. γ-H2AX enrichment also occurs as a response to the DNA fragmentation during apoptosis.[38]

To investigate whether DSBs underlie the G2/M arrest and apoptosis of Sc*Atrx*KO Sertoli cells, we performed co-IF for GATA4 and γ-H2AX (Figure 3A). In both control and Sc*Atrx*KO Sertoli cells, we observed two different types of γ-H2AX staining patterns in Sertoli cells with GATA4 foci. γ-H2AX showed either localized staining (L) at the GATA4 foci only (Figures 3A and 3B, blue slices in pie charts) or both localized and widespread (LW) throughout the nucleus, indicative of the cell undergoing apoptosis (Figures 3A and 3B, orange slices in pie charts). In control testes, around 10% of the Sertoli cells with GATA4 foci showed prominent γ-H2AX staining (4.1% localized and 6.2% widespread) (Figure 3B). Sc*Atrx*KO Sertoli cells with regular sized GATA4 foci showed similar widespread γ-H2AX staining (5.8%), but localized γ-H2AX staining was increased by almost 11-fold (43.7%) (Figure 3B). Remarkably, all G2/M-arrested Sertoli cells with the giant GATA4 foci were γ-H2AX-positive with 51.7% and 48.3% of them showing localized and widespread γ-H2AX-staining, respectively (Figure 3B). To confirm the presence of DSBs at the GATA4 foci we also performed co-IF for the chromatin-binding p53-binding protein 1 (53BP1) which is an important regulator of DSB signaling by recruiting DSB signaling and repair proteins to the damaged site and promoting end joining of distal DNA ends.[39] Indeed, while 53BP1 staining was present at the GATA4 foci in Sertoli cells of Sc*Atrx*KO testes, it was not detectable in control testes (Figure S2).

Taken together, these data indicate that loss of ATRX at the GATA4 foci leads to local DNA damage followed by apoptosis of the G2/M-arrested Sertoli cells with giant GATA4 foci, possibly due to the failure of DNA repair.

Table 2. Percentage of PML-positive GATA4 foci in control and Sc*Atrx*KO testes

	Control	KO	
Animals	*n* = 3	*n* = 3	
Number of Sertoli cells with single GATA4 foci	119	216 (regular)	35 (giant)
PML-positive GATA4 foci	20	166 (regular)	33 (giant)
Percentage: PML-positive GATA4 foci	**16.8%**	**76.9% (regular)**	**94.3% (giant)**

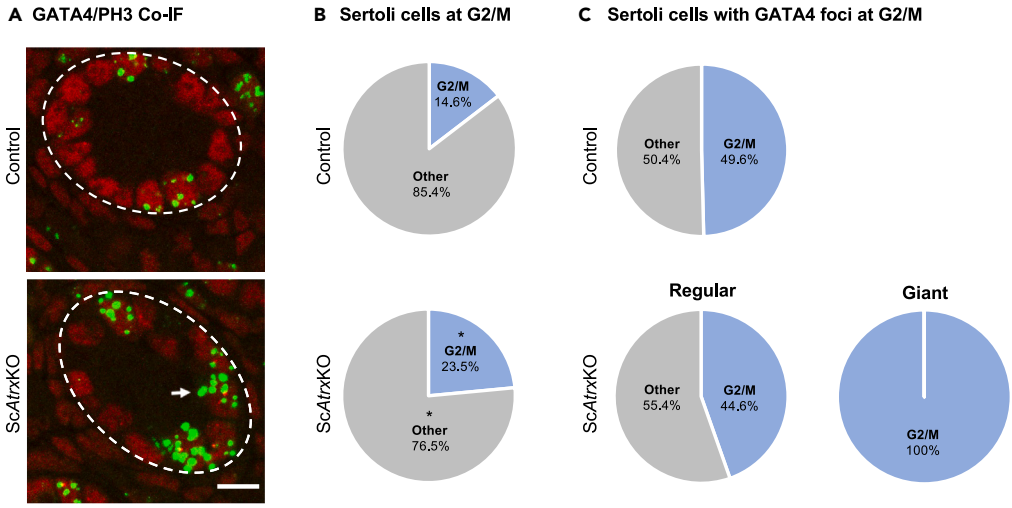

Figure 2. ScAtrxKO Sertoli cells with giant GATA4 foci are arrested at G2/M

(A) Double immunofluorescence (IF) analyses in E16.5 XY control and ScAtrxKO testes for GATA4 (red, nuclear) and PH3 (green, nuclear), a marker of late G2 phase and mitosis. Dashed lines mark the basal lamina of the testis cords. The white arrow denotes a Sertoli cell with a giant GATA4 speckle. Scale bar represents 10 μm.

(B) Pie charts showing the percentages of the cell cycle stages in Sertoli cells of E16.5 XY control and ScAtrxKO testes. More than 2,000 and 1,000 Sertoli cells were counted in $n = 2$ control and $n = 3$ ScAtrxKO testes, respectively. *$p < 0.05$, one-way ANOVA.

(C) Pie charts showing the percentages of the cell-cycle stages in Sertoli cells with GATA4 foci of E16.5 XY control and ScAtrxKO testes. More than 200 Sertoli cells with GATA4 foci were analyzed in $n = 2$ control and $n = 3$ ScAtrxKO testes.

GATA4 foci represent sites of early chromosome condensation that require ATRX

Phosphorylation of histone 3 is required for the initiation of chromosome condensation.[40] H3 phosphorylation initiates at the pericentromeric heterochromatin of the chromosomes (bright DAPI regions) during G2 phase, then spreads toward the chromosome arms and is complete by mitotic prophase.[36] Surprisingly, our co-IF analyses for GATA4 and PH3 revealed that PH3 staining was not only found at the bright DAPI regions but also at the GATA4 foci (Figure 4A). In PH3-positive control Sertoli cells, 86% of GATA4 foci were PH3 positive (Figure 4B). However, in PH3-positive ScAtrxKO Sertoli cells, only 52% of the regular sized GATA4 foci were also positive for PH3, whereas no PH3 staining was detected at the giant GATA4 foci in G2/M-arrested Sertoli cells (Figures 4A and 4B). In contrast, H3 phosphorylation at the bright DAPI regions in ScAtrxKO Sertoli cells was unaffected (Figure 4A, yellow arrowheads). These data suggest that like the chromocenters, the GATA4 foci might represent sites of early chromosome condensation. They also suggest that loss of ATRX in Sertoli cells results in a failure of chromosome condensation at the GATA4 foci but not at the chromocenters.

We next looked for potential structural similarities between the GATA4 foci and chromocenters. A characteristic feature of each chromocenter is the presence of highly compacted HP1α-positive pericentromeric heterochromatin (major satellites) of multiple chromosomes, while the corresponding centromeres (minor satellites) closely surround the chromocenters as several separate structures.[35] Indeed, co-IF analyses in control Sertoli cells for GATA4 and HP1α, a hallmark of pericentromeric heterochromatin, revealed that 79% of GATA4 foci are HP1α-positive (Figure 5). This suggests that HP1α is recruited to the GATA4 foci and that the GATA4 foci, like the chromocenters, contain highly compacted heterochromatin. However, in ScAtrxKO testes, HP1α staining was either severely reduced or absent at the GATA4 foci. (Figure 5), suggesting that heterochromatin formation at these foci is perturbed in the absence of ATRX. In contrast, HP1α staining at pericentromeric heterochromatin (bright DAPI regions) in ScAtrxKO testes was unaffected (Figure 5, yellow arrowheads). Co-IF for GATA4 and the centromeric protein CENPA, which is found at all centromeres, revealed a single signal in close association with the GATA4 foci in both control and ScAtrxKO Sertoli cells (Figure 6A, left images). Furthermore, co-IF for GATA4 and TERF1, a telomere marker, revealed two telomere signals closely associated with the GATA4 foci of control and ScAtrxKO Sertoli cells (Figure 6A, right images).

Taken together, the GATA4 foci show structural and functional similarities to chromocenters (Presence of HP1α, PH3, and centromere in close association), but unlike chromocenters they appear to contain only chromatin from a single chromosome.

GATA4 foci contain the Yp

Recently, it has been demonstrated that a 300 kb region (YS300) on the Yp is frequently associated with a large PML NB in mouse embryonic stem cells (mESCs).[29] Therefore, we investigated whether the single chromosome at the GATA4 foci may be the Y chromosome. We performed immunofluorescence *in situ* hybridization (Immuno-FISH) for GATA4 and two different Y probes, a 73.6 kb Yp probe (Chr Y: 112,036–184,662) that detects the 300 kb region associated with the reported PML NB[29] and a Yq probe that detects a 1.8 kb repeat dispersed over a 48 Mb region across the long arm of the Y chromosome (Chr Y: 4,173,195–52,194,425).[41,42] Immuno-FISH for GATA4 and the Yp probe

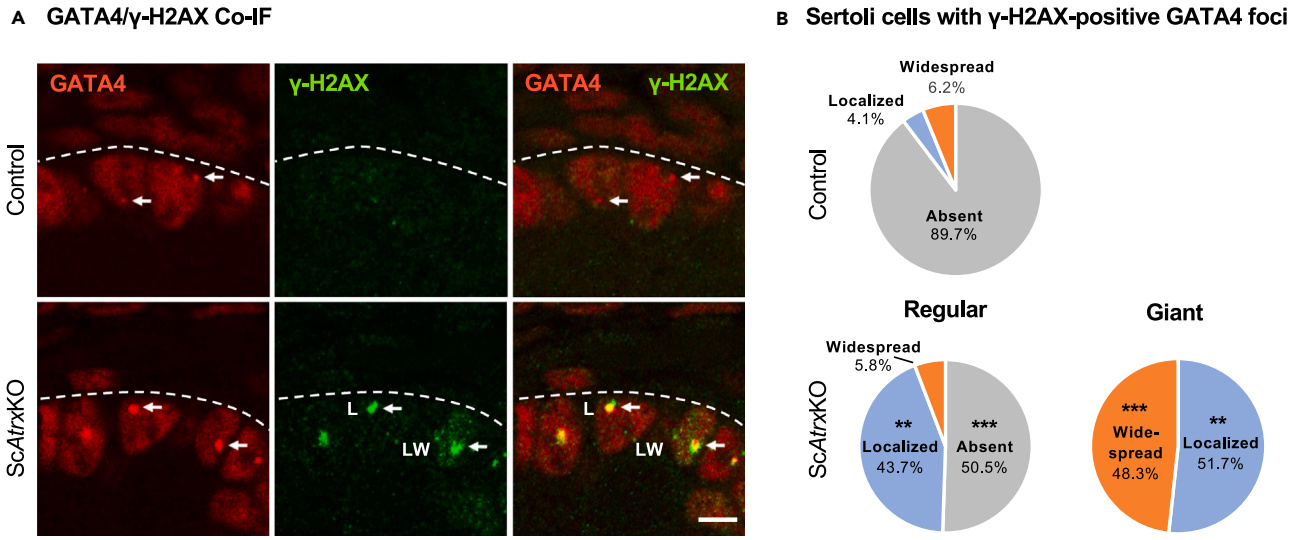

Figure 3. Loss of ATRX at the GATA4 foci leads to DNA double-strand breaks

(A) Double immunofluorescence (IF) analyses in E16.5 XY control and Sc*Atrx*KO testes for GATA4 (red, nuclear) and γ-H2AX (green, nuclear), a marker of DNA double-strand breaks and apoptosis. White arrows denote GATA4 foci. L, localized γ-H2AX staining specifically at the GATA4 foci; LW, localized and widespread γ-H2AX staining throughout the nucleus, indicative of the Sertoli cell undergoing apoptosis. Dashed lines mark the basal lamina of the testis cords. Scale bar represents 5 μm.

(B) Pie charts showing the percentages of γ-H2AX-positive GATA4 foci in Sertoli cells of E16.5 XY control and Sc*Atrx*KO testes. More than 200 Sertoli cells with GATA4 foci were analyzed in $n = 2$ control and $n = 3$ Sc*Atrx*KO testes. $^{**}p < 0.01$, $^{***}p < 0.001$; one-way ANOVA.

See also Figure S2.

revealed that Yp co-localized completely or partially with the GATA4 signal in 81% of control and 93% of Sc*Atrx*KO Sertoli cells (Figure 6Bi). In contrast, the signal of the Yq probe was often close to but did not co-localize with the GATA4 signal (Figure 6Bii). Taken together, these data indicate that the GATA4 foci locate to the short arm of the Y chromosome.

Yp is enriched for GATA repeats and contains potential G4 DNA structures

Given the co-localization of the GATA4 foci with Yp, we wondered whether the Yp probe sequence contains potential ATRX and GATA4 binding sites. The GATA4 foci show intense staining, suggesting that large numbers of GATA4 proteins are present at these sites. It is therefore possible that GATA4 is binding repetitively to chromatin, unlike in its role as a transcription factor where it binds only once.[43] The GATA family binds to the sequence motif "T/A(GATA)A/G" with AGATAG being the most preferred.[44] Sex chromosomes contain highly conserved banded krait minor (Bkm) satellite DNA sequences in which GATA repeats are the major component. Intriguingly, in the mouse, these GATA repeats are predominantly confined to the short arm of the Y chromosome.[45–47] Analysis of the entire 73.6 kb Yp probe sequence revealed a ~4.6 kb region with a high accumulation of GATA repeats of which the most abundant is the preferred GATA4 binding site "AGA TAG" (Figure 7A). In contrast, the weaker GATA family binding sites "C/G(GATA)T/C" are present in low numbers and are evenly distributed throughout the Yp sequence (Figure 7B). ATRX binds to G-quadruplex DNA secondary structures (G4) that are formed by G-rich tandem repeats such as the telomeric repeat TTAGGG.[48] The G4 DNA sequences consist of four interrupted stretches of at least three guanines which form a four-stranded DNA secondary structure that is stabilized by G-quartets. Using QGRS Mapper,[49] we identified 8 putative G4-sequences with a G-score threshold ≥22 (Table 3). These data show that the 73.6 kb Yp probe sequence contains potential binding sites for both GATA4 and ATRX.

DISCUSSION

In this study, we have identified a vulnerability of Sertoli cells during fetal development. We show that loss of ATRX in mouse Sertoli cells results in severe local defects, DNA double-strand breaks and loss of the chromatin marks HP1α and PH3, at a novel giant GATA4 PML-NB on the short arm of the Y chromosome. In contrast, the vast majority of studies in ATRX-deficient mouse cell lines or tissues such as the brain, mESCs, and oocytes showed that defects like DSBs at telomeres or loss of PH3 at pericentromeric heterochromatin occur across all chromosomes.[8,12,50] The reason is that the chromosomal sites, the telomeres and pericentromeric heterochromatin, where ATRX binds to and is important in these other tissues, are highly conserved in mouse chromosomes.[35] Therefore, loss of ATRX in these tissues will lead to chromosome-wide defects. In mice, a specific PML NB can directly interact with Yp was recently demonstrated in mESCs.[29] In these cells, a 300 kb region (YS300) near the Y chromosome telomere that contains the Yp probe used in our study is frequently associated with a large PML NB.[29] This PML NB forms a specific complex with YS300 to regulate the expression of neighboring clustered genes such as *Uty* and *Ddx3y*. However,

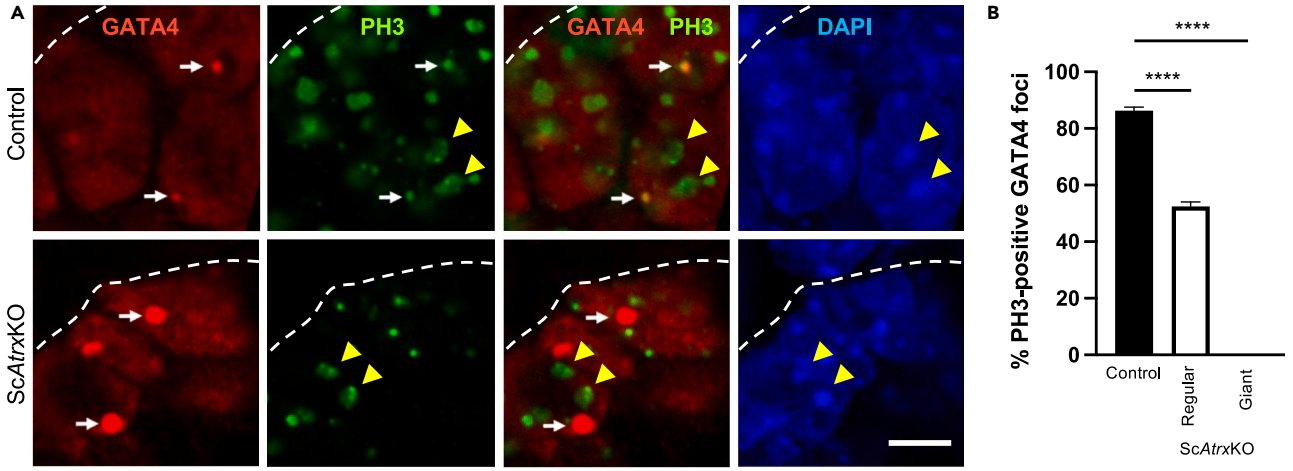

Figure 4. GATA4 foci are a site of early chromosome condensation that requires ATRX

(A) Double immunofluorescence (IF) analyses in E16.5 XY control and Sc*Atrx*KO testes for GATA4 (red, nuclear) and PH3 (green, nuclear), a marker of late G2 phase and mitosis. DAPI (blue) was used as a nuclear stain. White arrows show GATA4 foci; yellow arrowheads denote PH3-positive pericentromeric heterochromatin (bright DAPI regions); Dashed lines mark the basal lamina of the testis cords; Scale bar represents 5 μm.

(B) Percentage of PH3-positive GATA4 foci in Sertoli cells of E16.5 XY control and Sc*Atrx*KO testes. More than 200 Sertoli cells with GATA4 foci were analyzed in $n = 2$ control and $n = 3$ Sc*Atrx*KO testes. Values are the mean ± SEM. ****$p < 0.0001$, One-way ANOVA.

the Yp-linked PML NB in Sertoli cells must serve a different function because these Y-linked genes are spermatogenesis genes and thus are not expressed in Sertoli cells.

Why does a GATA4 PML-NB form on Yp in Sertoli cells? All GATA4 foci in control Sertoli cells contain ATRX, DAXX, GATA4, and FOG2, whereas only a subset of GATA4 foci contains HP1α (79%) and PML (17%). This indicates that ATRX, DAXX, GATA4, and FOG2 form a core unit on chromatin which is followed by the recruitment of HP1α and PML. PML is recruited during G2 since almost all the giant GATA4 foci in G2/M-arrested Sertoli cells were positive for PML. DAXX can target ATRX to PML NBs,[7,51] and vice versa, we observed that ATRX is required for expression of DAXX at the PML NBs. Moreover, we found that in Sertoli cells, ATRX is required for localization of HP1α to PML NBs. This is consistent with a previous observation during neural differentiation where ATRX plays a role in targeting HP1α to pericentromeric heterochromatin.[6] ATRX itself might bind to the potential G4 DNA sequences present within Yp. Since PML interacts with and can recruit DAXX to PML NBs,[52] DAXX might also be involved in the recruitment of PML to the GATA4 foci. However, we speculate that the GATA4 foci play a unique role in PML NB formation specifically at Yp. GATA4 is highly expressed throughout the nucleus and is a DNA sequence-specific transcription factor with important functions in testis and heart development.[33,34,53] It was therefore surprising to identify an intense focal accumulation of GATA4 within the nucleus. GATA4 has never been reported to be present within PML NBs, suggesting a novel structural role.[26–28] Similarly, its partner protein FOG2 represents a novel protein within PML NBs. One unique feature of the short arm of the mouse Y chromosome is the presence of the evolutionarily conserved Bkm satellite DNA sequences in which GATA repeats are the major component.[45–47] Indeed, we found that the 73.6 kb Yp probe contains a ~4.6 kb region with a high accumulation of these GATA repeats. GATA4 could bind repetitively to this region and act as a docking site for PML NB formation. In support of the latter point, GATA2, another member of the GATA family of transcription factors, is one of over 250 proteins associated with PML NBs.[27] Since GATA2 can interact with the PML protein via its zinc finger region shared by all GATA proteins,[54] GATA4 may also interact with PML. Another unique feature of Yp is the presence of specific inverted repeats within YS300 that are not homologous to other sequences in the genome.[29] It is possible that these sequences may also play a unique role in the formation of a PML NB specifically at this chromosomal region. In support of this, ATRX has been shown to associate with Y chromosome-specific repeat sequences in male mouse primary embryonic fibroblasts (MEFs).[55]

One major defect in Sc*Atrx*KO Sertoli cells is the formation of DSBs, as indicated by the presence of γ-H2AX and 53BP1 at a specific HP1α-positive heterochromatic region on Yp that is associated with the GATA4 PMLNB. DSBs result from replication stress at chromosomal regions that are difficult to replicate, including common fragile sites, pericentromeric heterochromatin, and telomeres, to which ATRX all binds.[5,56,57] The expanded repeats in common fragile sites and telomeres form DNA secondary structures such as hairpins (at common fragile sites) and G4 structures (at common fragile sites and telomeres) that can lead to replication fork stalling or collapse with consequent generation of DSBs.[48,58] ATRX is a crucial factor in common fragile sites, pericentromeric heterochromatin, and telomere stability. ATRX facilitates replication by preventing G4 structure formation and promotes replication fork recovery and HR-dependent repair of DSBs.[5,8,12–16] Therefore, one major role of ATRX at the GATA4 PML-NB could be to protect a specific HP1α-positive heterochromatic region on Yp that is vulnerable to DNA damage during replication. However, it remains unknown what makes this region on Yp so fragile. The Yp probe sequence contains several putative G4-sequences, therefore, like at telomeres, ATRX may be involved in preventing G4 DNA structures. It is also possible that the Yp-specific GATA repeats represent a common fragile site that ATRX helps to stabilize and thereby prevent DSBs at Yp. In support of this, a major class of common fragile sites are interrupted runs of AT-dinucleotides that can form secondary structures.[58] Of interest, the

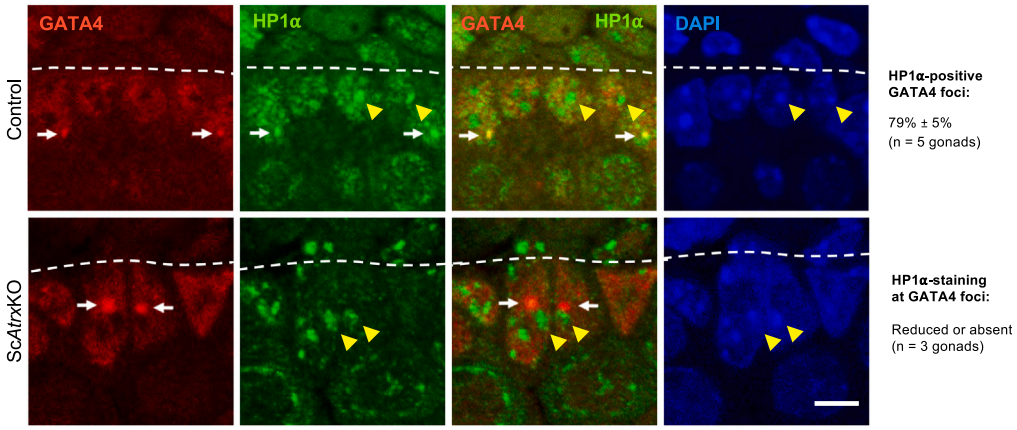

Figure 5. ScAtrxKO Sertoli cells show specific loss of HP1α at the GATA4 foci

Double immunofluorescence (IF) analyses in E16.5 XY control and ScAtrxKO testes for GATA4 (red, nuclear) and HP1α (green, nuclear), a marker of highly compacted heterochromatin. DAPI (blue) was used as a nuclear stain. White arrows show GATA4 foci; yellow arrowheads denote HP1α-positive pericentromeric heterochromatin (bright DAPI regions); Dashed lines mark the basal lamina of the testis cords. Scale bar represents 5 μm.

DNA damage (single γ-H2AX foci) in ScAtrxKO Sertoli cells at the single GATA4 foci often occurs close to the nuclear periphery analogous to mice with conditional knockout of *Atrx* in the limb mesenchyme which also show single γ-H2AX foci close to the nuclear lamina, although those mechanisms remain elusive.[59]

A second major defect at the GATA4 PML-NBs in Sertoli cells of ScAtrxKO mice is the loss of HP1α and PH3, indicating changes in chromatin structure and abnormal chromosome condensation, respectively. The GATA4 foci show some structural and functional similarities to chromocenters. Chromocenters are the bright DAPI regions in the nucleus that contain the pericentromeric heterochromatin of several chromosomes.[35] Pericentromeric heterochromatin which is composed of major satellite DNA represents the initiation sites for chromosome condensation, marked by early phosphorylation of histone H3 during G2.[36] ATRX locates to pericentromeric heterochromatin[56] and mediates its establishment and maintenance through deposition of H3.3, together with DAXX within PML NBs, and recruitment of HP1α.[6,11] Moreover, in mouse oocytes, loss of ATRX leads to reduced phosphorylation of histone H3 at pericentromeric heterochromatin associated with incomplete chromosome condensation and centromeric breaks.[50] In Sertoli cells, we found that ATRX is expressed not only at the HP1α-positive pericentromeric heterochromatin as expected but also strongly at the HP1α-positive heterochromatin region at the GATA4 foci on Yp. Strikingly, this region is often in very close association with one of the chromocenters. Like the chromocenters, this region contains ATRX, DAXX, HP1α, and PML. Moreover, although the Y chromosome lacks the major satellite DNA of the autosomes,[60] the HP1α-positive Yp heterochromatin region also shows early phosphorylation of histone H3 during G2. Therefore, the GATA4 foci may represent a starting point for Yp-chromosome condensation. Alternatively, the early enrichment of PH3 may simply reflect the fact that heterochromatin generally condenses early.[61] Despite the reported roles for ATRX at pericentromeric heterochromatin, prominent γ-H2AX staining and loss of HP1α and PH3 in ScAtrxKO mice were only observed at the GATA4 foci and not at the chromocenters. This underscores the multiple roles of ATRX during development where its importance depends on the specific tissue context.

The chromatin defects in the G2/M arrested Sertoli cells of ScAtrxKO mice are associated with the occurrence of single giant PML NBs. Intriguingly, single giant PML NBs generated during the G2 phase have been reported once before in a genetic disease, the immunodeficiency, centromeric region instability, facial anomalies syndrome (ICF) caused by mutations in the DNA methyltransferase gene *DNMT3B*.[62–64] DNMT3B is involved in the methylation of GC-rich major satellites that are predominantly located at the pericentromeric heterochromatin of chromosomes 1 and 16 (satellite 2 DNA) and chromosome 9 (satellite 3 DNA). *DNMT3B* mutations lead to hypomethylation, decondensation, and instability of these major satellites, resulting in chromosome breaks. The giant PML NBs in ICF cells consist of ATRX, DAXX, HP1α, and several other proteins and contain the major satellites of all three chromosomes. It was therefore proposed that these PML NBs promote the condensation of these satellites specifically at G2 phase before mitosis. The authors also concluded that the giant PML NBs in ICF syndrome patients are most likely due to the undercondensed satellite DNA occupying a larger space compared to the condensed state. Given these data and the absence of HP1α and PH3 at the giant GATA4 PML-NBs in ScAtrxKO Sertoli cells, it is likely that the Yp region occupied by the giant PML NB is also undercondensed and that the GATA4 PML-NBs become giant due to chromatin expansion. It is also possible that in the uncondensed chromatin, the high affinity GATA sites at Yp become more accessible, resulting in increased recruitment of GATA4. Moreover, because GATA4 and PML are recruited during G2, the G2 arrest of ScAtrxKO Sertoli cells could lead to ongoing recruitment of these proteins, thus contributing to the enlargement of the GATA4 PML-NBs. Overall, these data indicate that the PML NB associated with chromosomes 1, 9, and 16 in humans and the PML NB associated with the Y chromosome in mice show functional similarities. Therefore, a major role of ATRX at the GATA4 PML-NB may be to maintain the heterochromatic state and to promote condensation of the HP1α-positive heterochromatic region on Yp.

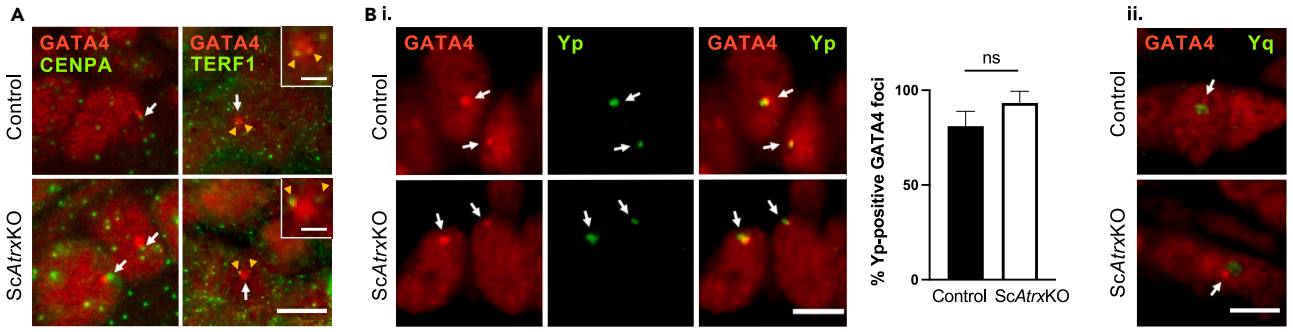

Figure 6. GATA4 foci contain the Y chromosome short arm (Yp)

(A) *Left images:* Double immunofluorescence (IF) analyses in E16.5 XY control and Sc*Atrx*KO testes for GATA4 (red, nuclear) and CENPA (green, nuclear), a centromere marker. *Right images*: Double IF analyses in E16.5 XY control and Sc*Atrx*KO testes for GATA4 (red, nuclear) and TERF1 (green, nuclear), a telomere marker. The insets show magnifications of the GATA4 foci.

(B) (i) Immuno-FISH for GATA4 and a Yp probe. Yp co-localized completely or partially with the GATA4 signal in 81% of control and 93% of Sc*Atrx*KO Sertoli cells. More than 150 Sertoli cells with GATA4 foci were analyzed in control and Sc*Atrx*KO testes. Values are the mean ± SEM (n = 3 gonads). Ns; not significant; two tailed t test compared to control. (ii) Immuno-FISH for GATA4 and a Yq probe. Scale bars represent 5 μm; Scale bars in insets represent 1 μm.

See also Table S3.

The occurrence of two major defects at the GATA4 PML-NBs of Sc*Atrx*KO mice, DSB formation and a failure of chromosome condensation, could reflect distinct roles for ATRX in Sertoli cells. However, it is also possible that ATRX is not directly required for recruitment of HP1α and phosphorylation of histone H3 at the GATA4 foci and that the chromatin structure and condensation defects are a consequence of the DNA double-strand breaks. Indeed, DNA damage response can result in dynamic changes in chromatin structure, for example, experimental induction of double-stranded breaks in mammalian cells leads to local chromatin decondensation.[65–67]

Based on our findings, we propose that in Sc*Atrx*KO mice, DSBs are generated at a fragile Yp heterochromatic region within a dysfunctional PML NB. This will trigger the phosphorylation of the histone variant H2AX which is known to recruit DNA repair proteins and induce G2/M cell-cycle arrest.[37,38] Either as an independent event within the dysfunctional PML NB or due to the DSBs, the heterochromatic state of the Yp region is not maintained which fails to condense, resulting in an expansion of the PML NB (giant PML NB). All Sertoli cells with giant PML NBs were arrested at G2/M and showed γ-H2AX-staining on their giant PML NBs, about half of them also showed widespread γ-H2AX-staining. These observations directly link chromosome decondensation and DSBs to the observed G2/M arrest and apoptosis in Sc*Atrx*KO mice. The fact that DSBs predominantly occur at Yp in the absence of ATRX is consistent with our observation that ATRX, a guardian of chromatin, is most strongly expressed at the Yp-located GATA PML NBs in Sertoli cells. For other chromosomal regions prone to DSBs, other proteins within the PML-NB multiprotein complex could protect chromatin.

In summary, our data indicate that DNA damage and a failure of chromosome condensation at the short arm of the Y chromosome underlie the testicular abnormalities in ATR-X syndrome. This establishes Y chromosome damage as a novel mechanism for testicular failure.

Limitations of the study

Although we provide a comprehensive discussion of how the GATA4 PML-NB might form on Yp in Sertoli cells, what makes Yp so fragile and how ATRX prevents and/or repairs the DSBs at Yp, these questions still need to be answered in future studies. In addition, further investigation is required to determine whether Y chromosome damage also occurs in other ATRX-deficient tissues or whether it is specific to Sertoli cells.

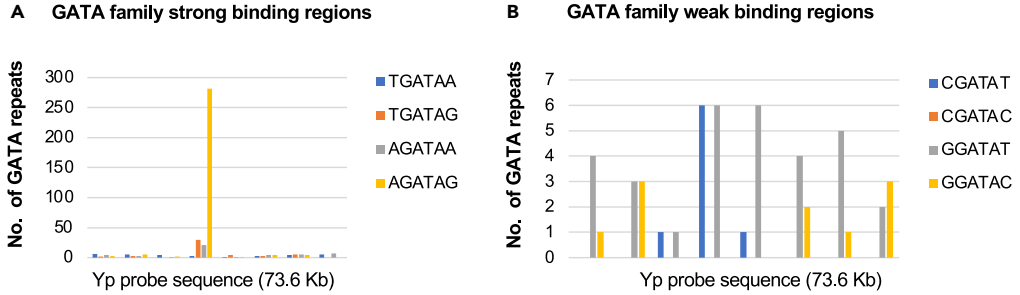

Figure 7. Yp is enriched for GATA repeats

(A) The 73.6 kb Yp probe contains a 4.6. kb region that is enriched for the strong GATA family binding site "AGATAG".

(B) The GATA family poor binding sites, "C/G(GATA)T/C," are present at low numbers within the Yp probe sequence.

Table 3. Identification of putative G4-sequences within the Yp probe using QGRS Mapper

Position	Length	QGRS	G-score
3465	26	**GGG**GT**GGG**AGCTA**GGG**AGGCGAT**GGG**	37
18160	25	**GGG**CCAAAAA**GGG**GGAGT**GGG**C**GGG**	36
18188	27	**GGG**AGTGG**GGG**TGTGT**GGG**TATGG**GGG**	42
44685	26	**GGG**CT**GGG**CGAAGT**GGG**AGTGCT**GGG**	38
51330	26	**GGG**CAT**GGG**GAG**GGG**AGGTAAGA**GGG**	37
66213	29	**GGG**GGAGT**GGG**TGGGTA**GGG**GATTGT**GGG**	41
69010	21	**GGG**AAGCAA**GGG**A**GGG**CA**GGG**	37
72718	19	**GGGG**T**GGGG**T**GGGG**T**GGGG**	63

The four G-tracts in each of the eight putative G4-sequences are in bold and underlined. A higher G-score indicates a higher likelihood to form an unimolecular quadruplex.

STAR★METHODS

Detailed methods are provided in the online version of this paper and include the following:

- KEY RESOURCES TABLE
- RESOURCE AVAILABILITY
  - Lead contact
  - Materials availability
  - Data and code availability
- EXPERIMENTAL MODEL AND STUDY PARTICIPANT DETAILS
  - Mice and ethics
  - Tissue processing and paraffin sectioning
- METHOD DETAILS
  - Immunofluorescence
  - Preparation of BAC DNA
  - Immuno-FISH
- QUANTIFICATION AND STATISTICAL ANALYSIS
  - Quantification of cell numbers
  - Measurement of GATA4 foci diameter
  - Statistical analysis

SUPPLEMENTAL INFORMATION

Supplemental information can be found online at https://doi.org/10.1016/j.isci.2024.109629.

ACKNOWLEDGMENTS

We thank Monash Medical Imaging, Monash Histology, Helena Sim, Janelle Ryan, Sophia Astbury, Kerryn Bird, and Karisma Lawrence for technical assistance, Yusuke Miyanari and Paul Kalitsis for providing the Yp and Yq probes, respectively, and Florian Guillou for *AMH-Cre* mice and Doug Higgs for the *Atrx*$^{flox/flox}$ mice.

National Health and Medical Research Council (NHMRC, Australia) program grant 1074258; NHMRC project grant 1004992; Victorian Government's Operational Infrastructure Support Program; NHMRC Research Fellowship 441102.

AUTHOR CONTRIBUTIONS

Conceptualization, S.B.-F. and V.R.H.; methodology, N.L.C., A.G., L.H.W. and S.B.-F.; formal analysis, N.L.C.; investigation, N.L.C., T.N.U.L., and S.B.-F.; writing – original draft, N.L.C., T.N.U.L., and S.B.-F.; writing – review and editing, L.H.-W. and V.R.H.; funding acquisition, S.B.-F. and V.R.H.; resources, A.G., and L.H.-W.; visualization, N.L.C. and S.B.-F.; supervision, S.B.-F. and V.R.H.; project administration, S.B.-F. and V.R.H.

DECLARATION OF INTERESTS

The authors declare no competing interests.

Received: November 23, 2023
Revised: February 27, 2024
Accepted: March 26, 2024
Published: March 28, 2024

REFERENCES

1. Wilkie, A.O., Gibbons, R.J., Higgs, D.R., and Pembrey, M.E. (1991). X linked alpha thalassaemia/mental retardation: spectrum of clinical features in three related males. J. Med. Genet. *28*, 738–741. https://doi.org/10.1136/jmg.28.11.738.
2. Wilkie, A.O., Zeitlin, H.C., Lindenbaum, R.H., Buckle, V.J., Fischel-Ghodsian, N., Chui, D.H., Gardner-Medwin, D., MacGillivray, M.H., Weatherall, D.J., and Higgs, D.R. (1990). Clinical features and molecular analysis of the alpha thalassemia/mental retardation syndromes. II. Cases without detectable abnormality of the alpha globin complex. Am. J. Hum. Genet. *46*, 1127–1140.
3. Gibbons, R.J., and Higgs, D.R. (2000). Molecular-clinical spectrum of the ATR-X syndrome. Am. J. Med. Genet. *97*, 204–212. https://doi.org/10.1002/1096-8628(200023)97:3<204::Aid-ajmg1038>3.0.Co;2-x.
4. Gibbons, R.J., Wilkie, A.O., Weatherall, D.J., and Higgs, D.R. (1991). A newly defined X linked mental retardation syndrome associated with alpha thalassaemia. J. Med. Genet. *28*, 729–733. https://doi.org/10.1136/jmg.28.11.729.
5. Pladevall-Morera, D., Munk, S., Ingham, A., Garribba, L., Albers, E., Liu, Y., Olsen, J.V., and Lopez-Contreras, A.J. (2019). Proteomic characterization of chromosomal common fragile site (CFS)-associated proteins uncovers ATRX as a regulator of CFS stability. Nucleic Acids Res. *47*, 8004–8018. https://doi.org/10.1093/nar/gkz510.
6. Marano, D., Fioriniello, S., Fiorillo, F., Gibbons, R.J., D'Esposito, M., and Della Ragione, F. (2019). ATRX Contributes to MeCP2-Mediated Pericentric Heterochromatin Organization during Neural Differentiation. Int. J. Mol. Sci. *20*, 5371. https://doi.org/10.3390/ijms20215371.
7. Tang, J., Wu, S., Liu, H., Stratt, R., Barak, O.G., Shiekhattar, R., Picketts, D.J., and Yang, X. (2004). A novel transcription regulatory complex containing death domain-associated protein and the ATR-X syndrome protein. J. Biol. Chem. *279*, 20369–20377. https://doi.org/10.1074/jbc.M401321200.
8. Wong, L.H., McGhie, J.D., Sim, M., Anderson, M.A., Ahn, S., Hannan, R.D., George, A.J., Morgan, K.A., Mann, J.R., and Choo, K.H.A. (2010). ATRX interacts with H3.3 in maintaining telomere structural integrity in pluripotent embryonic stem cells. Genome Res. *20*, 351–360. https://doi.org/10.1101/gr.101477.109.
9. Xue, Y., Gibbons, R., Yan, Z., Yang, D., McDowell, T.L., Sechi, S., Qin, J., Zhou, S., Higgs, D., and Wang, W. (2003). The ATRX syndrome protein forms a chromatin-remodeling complex with Daxx and localizes in promyelocytic leukemia nuclear bodies. Proc. Natl. Acad. Sci. USA *100*, 10635–10640. https://doi.org/10.1073/pnas.1937626100.
10. Goldberg, A.D., Banaszynski, L.A., Noh, K.M., Lewis, P.W., Elsaesser, S.J., Stadler, S., Dewell, S., Law, M., Guo, X., Li, X., et al. (2010). Distinct factors control histone variant H3.3 localization at specific genomic regions. Cell *140*, 678–691. https://doi.org/10.1016/j.cell.2010.01.003.
11. Drané, P., Ouararhni, K., Depaux, A., Shuaib, M., and Hamiche, A. (2010). The death-associated protein DAXX is a novel histone chaperone involved in the replication-independent deposition of H3.3. Genes Dev. *24*, 1253–1265. https://doi.org/10.1101/gad.566910.
12. Watson, L.A., Solomon, L.A., Li, J.R., Jiang, Y., Edwards, M., Shin-ya, K., Beier, F., and Bérubé, N.G. (2013). Atrx deficiency induces telomere dysfunction, endocrine defects, and reduced life span. J. Clin. Invest. *123*, 2049–2063. https://doi.org/10.1172/jci65634.
13. Leung, J.W.C., Ghosal, G., Wang, W., Shen, X., Wang, J., Li, L., and Chen, J. (2013). Alpha thalassemia/mental retardation syndrome X-linked gene product ATRX is required for proper replication restart and cellular resistance to replication stress. J. Biol. Chem. *288*, 6342–6350. https://doi.org/10.1074/jbc.M112.411603.
14. Clynes, D., Jelinska, C., Xella, B., Ayyub, H., Taylor, S., Mitson, M., Bachrati, C.Z., Higgs, D.R., and Gibbons, R.J. (2014). ATRX dysfunction induces replication defects in primary mouse cells. PLoS One *9*, e92915. https://doi.org/10.1371/journal.pone.0092915.
15. Juhász, S., Elbakry, A., Mathes, A., and Löbrich, M. (2018). ATRX Promotes DNA Repair Synthesis and Sister Chromatid Exchange during Homologous Recombination. Mol. Cell *71*, 11–24.e7. https://doi.org/10.1016/j.molcel.2018.05.014.
16. Raghunandan, M., Yeo, J.E., Walter, R., Saito, K., Harvey, A.J., Ittershagen, S., Lee, E.A., Yang, J., Hoatlin, M.E., Bielinsky, A.K., et al. (2020). Functional cross talk between the Fanconi anemia and ATRX/DAXX histone chaperone pathways promotes replication fork recovery. Hum. Mol. Genet. *29*, 1083–1095. https://doi.org/10.1093/hmg/ddz250.
17. Salomoni, P., and Pandolfi, P.P. (2002). The role of PML in tumor suppression. Cell *108*, 165–170. https://doi.org/10.1016/s0092-8674(02)00626-8.
18. Bernardi, R., and Pandolfi, P.P. (2007). Structure, dynamics and functions of promyelocytic leukaemia nuclear bodies. Nat. Rev. Mol. Cell Biol. *8*, 1006–1016. https://doi.org/10.1038/nrm2277.
19. Lallemand-Breitenbach, V., and de Thé, H. (2010). PML nuclear bodies. Cold Spring Harb. Perspect. Biol. *2*, a000661. https://doi.org/10.1101/cshperspect.a000661.
20. Takahashi, Y., Lallemand-Breitenbach, V., Zhu, J., and de Thé, H. (2004). PML nuclear bodies and apoptosis. Oncogene *23*, 2819–2824. https://doi.org/10.1038/sj.onc.1207533.
21. Chang, H.R., Munkhjargal, A., Kim, M.J., Park, S.Y., Jung, E., Ryu, J.H., Yang, Y., Lim, J.S., and Kim, Y. (2018). The functional roles of PML nuclear bodies in genome maintenance. Mutat. Res. *809*, 99–107. https://doi.org/10.1016/j.mrfmmm.2017.05.002.
22. Bernardi, R., Papa, A., and Pandolfi, P.P. (2008). Regulation of apoptosis by PML and the PML-NBs. Oncogene *27*, 6299–6312. https://doi.org/10.1038/onc.2008.305.
23. Dellaire, G., Ching, R.W., Ahmed, K., Jalali, F., Tse, K.C.K., Bristow, R.G., and Bazett-Jones, D.P. (2006). Promyelocytic leukemia nuclear bodies behave as DNA damage sensors whose response to DNA double-strand breaks is regulated by NBS1 and the kinases ATM, Chk2, and ATR. J. Cell Biol. *175*, 55–66. https://doi.org/10.1083/jcb.200604009.
24. Melnick, A., Fruchtman, S., Zelent, A., Liu, M., Huang, Q., Boczkowska, B., Calasanz, M., Fernandez, A., Licht, J.D., and Najfeld, V. (1999). Identification of novel chromosomal rearrangements in acute myelogenous leukemia involving loci on chromosome 2p23, 15q22 and 17q21. Leukemia *13*, 1534–1538. https://doi.org/10.1038/sj.leu.2401513.
25. Weis, K., Rambaud, S., Lavau, C., Jansen, J., Carvalho, T., Carmo-Fonseca, M., Lamond, A., and Dejean, A. (1994). Retinoic acid regulates aberrant nuclear localization of PML-RAR alpha in acute promyelocytic leukemia cells. Cell *76*, 345–356. https://doi.org/10.1016/0092-8674(94)90341-7.
26. Dellaire, G., Farrall, R., and Bickmore, W.A. (2003). The Nuclear Protein Database (NPD): sub-nuclear localisation and functional annotation of the nuclear proteome. Nucleic Acids Res. *31*, 328–330. https://doi.org/10.1093/nar/gkg018.
27. Van Damme, E., Laukens, K., Dang, T.H., and Van Ostade, X. (2010). A manually curated network of the PML nuclear body interactome reveals an important role for PML-NBs in SUMOylation dynamics. Int. J. Biol. Sci. *6*, 51–67. https://doi.org/10.7150/ijbs.6.51.
28. Barroso-Gomila, O., Trulsson, F., Muratore, V., Canosa, I., Merino-Cacho, L., Cortazar, A.R., Pérez, C., Azkargorta, M., Iloro, I., Carracedo, A., et al. (2021). Identification of proximal SUMO-dependent interactors using SUMO-ID. Nat. Commun. *12*, 6671. https://doi.org/10.1038/s41467-021-26807-6.
29. Kurihara, M., Kato, K., Sanbo, C., Shigenobu, S., Ohkawa, Y., Fuchigami, T., and Miyanari, Y. (2020). Genomic Profiling by ALaP-Seq Reveals Transcriptional Regulation by PML Bodies through DNMT3A Exclusion. Mol. Cell *78*, 493–505.e8. https://doi.org/10.1016/j.molcel.2020.04.004.
30. Ion, A., Telvi, L., Chaussain, J.L., Galacteros, F., Valayer, J., Fellous, M., and McElreavey, K. (1996). A novel mutation in the putative DNA helicase XH2 is responsible for male-to-female sex reversal associated with an atypical form of the ATR-X syndrome. Am. J. Hum. Genet. *58*, 1185–1191.
31. Bagheri-Fam, S., Argentaro, A., Svingen, T., Combes, A.N., Sinclair, A.H., Koopman, P., and Harley, V.R. (2011). Defective survival of proliferating Sertoli cells and androgen receptor function in a mouse model of the ATR-X syndrome. Hum. Mol. Genet. *20*, 2213–2224. https://doi.org/10.1093/hmg/ddr109.
32. Schindelin, J., Arganda-Carreras, I., Frise, E., Kaynig, V., Longair, M., Pietzsch, T., Preibisch,

S., Rueden, C., Saalfeld, S., Schmid, B., et al. (2012). Fiji: an open-source platform for biological-image analysis. Nat. Methods *9*, 676–682. https://doi.org/10.1038/nmeth.2019.

33. Manuylov, N.L., Zhou, B., Ma, Q., Fox, S.C., Pu, W.T., and Tevosian, S.G. (2011). Conditional ablation of Gata4 and Fog2 genes in mice reveals their distinct roles in mammalian sexual differentiation. Dev. Biol. *353*, 229–241. https://doi.org/10.1016/j.ydbio.2011.02.032.
34. Tevosian, S.G., Albrecht, K.H., Crispino, J.D., Fujiwara, Y., Eicher, E.M., and Orkin, S.H. (2002). Gonadal differentiation, sex determination and normal Sry expression in mice require direct interaction between transcription partners GATA4 and FOG2. Development *129*, 4627–4634. https://doi.org/10.1242/dev.129.19.4627.
35. Guenatri, M., Bailly, D., Maison, C., and Almouzni, G. (2004). Mouse centric and pericentric satellite repeats form distinct functional heterochromatin. J. Cell Biol. *166*, 493–505. https://doi.org/10.1083/jcb.200403109.
36. Hendzel, M.J., Wei, Y., Mancini, M.A., Van Hooser, A., Ranalli, T., Brinkley, B.R., Bazett-Jones, D.P., and Allis, C.D. (1997). Mitosis-specific phosphorylation of histone H3 initiates primarily within pericentromeric heterochromatin during G2 and spreads in an ordered fashion coincident with mitotic chromosome condensation. Chromosoma *106*, 348–360. https://doi.org/10.1007/s004120050256.
37. Plesca, D., Mazumder, S., and Almasan, A. (2008). DNA damage response and apoptosis. Methods Enzymol. *446*, 107–122. https://doi.org/10.1016/s0076-6879(08)01606-6.
38. Rogakou, E.P., Nieves-Neira, W., Boon, C., Pommier, Y., and Bonner, W.M. (2000). Initiation of DNA fragmentation during apoptosis induces phosphorylation of H2AX histone at serine 139. J. Biol. Chem. *275*, 9390–9395. https://doi.org/10.1074/jbc.275.13.9390.
39. Panier, S., and Boulton, S.J. (2014). Double-strand break repair: 53BP1 comes into focus. Nat. Rev. Mol. Cell Biol. *15*, 7–18. https://doi.org/10.1038/nrm3719.
40. Van Hooser, A., Goodrich, D.W., Allis, C.D., Brinkley, B.R., and Mancini, M.A. (1998). Histone H3 phosphorylation is required for the initiation, but not maintenance, of mammalian chromosome condensation. J. Cell Sci. *111* (Pt 23), 3497–3506. https://doi.org/10.1242/jcs.111.23.3497.
41. Udugama, M., Vinod, B., Chan, F.L., Hii, L., Garvie, A., Collas, P., Kalitsis, P., Steer, D., Das, P.P., Tripathi, P., et al. (2022). Histone H3.3 phosphorylation promotes heterochromatin formation by inhibiting H3K9/K36 histone demethylase. Nucleic Acids Res. *50*, 4500–4514. https://doi.org/10.1093/nar/gkac259.
42. Soh, Y.Q.S., Alföldi, J., Pyntikova, T., Brown, L.G., Graves, T., Minx, P.J., Fulton, R.S., Kremitzki, C., Koutseva, N., Mueller, J.L., et al. (2014). Sequencing the mouse Y chromosome reveals convergent gene acquisition and amplification on both sex chromosomes. Cell *159*, 800–813. https://doi.org/10.1016/j.cell.2014.09.052.
43. Bouchard, M.F., Bergeron, F., Grenier Delaney, J., Harvey, L.M., and Viger, R.S. (2019). In Vivo Ablation of the Conserved GATA-Binding Motif in the Amh Promoter Impairs Amh Expression in the Male Mouse. Endocrinology *160*, 817–826. https://doi.org/10.1210/en.2019-00047.
44. Merika, M., and Orkin, S.H. (1993). DNA-binding specificity of GATA family transcription factors. Mol. Cell Biol. *13*, 3999–4010. https://doi.org/10.1128/mcb.13.7.3999-4010.1993.
45. Singh, L., and Jones, K.W. (1982). Sex reversal in the mouse (Mus musculus) is caused by a recurrent nonreciprocal crossover involving the x and an aberrant y chromosome. Cell *28*, 205–216. https://doi.org/10.1016/0092-8674(82)90338-5.
46. Singh, L., Panicker, S.G., Nagaraj, R., and Majumdar, K.C. (1994). Banded krait minor-satellite (Bkm)-associated Y chromosome-specific repetitive DNA in mouse. Nucleic Acids Res. *22*, 2289–2295. https://doi.org/10.1093/nar/22.12.2289.
47. Singh, L., Phillips, C., and Jones, K.W. (1984). The conserved nucleotide sequences of Bkm, which define Sxr in the mouse, are transcribed. Cell *36*, 111–120. https://doi.org/10.1016/0092-8674(84)90079-5.
48. Wang, Y., and Patel, D.J. (1992). Guanine residues in d(T2AG3) and d(T2G4) form parallel-stranded potassium cation stabilized G-quadruplexes with anti glycosidic torsion angles in solution. Biochemistry *31*, 8112–8119. https://doi.org/10.1021/bi00150a002.
49. Kikin, O., D'Antonio, L., and Bagga, P.S. (2006). QGRS Mapper: a web-based server for predicting G-quadruplexes in nucleotide sequences. Nucleic Acids Res. *34*, W676–W682. https://doi.org/10.1093/nar/gkl253.
50. Baumann, C., Viveiros, M.M., and De La Fuente, R. (2010). Loss of maternal ATRX results in centromere instability and aneuploidy in the mammalian oocyte and pre-implantation embryo. PLoS Genet. *6*, e1001137. https://doi.org/10.1371/journal.pgen.1001137.
51. Ishov, A.M., Vladimirova, O.V., and Maul, G.G. (2004). Heterochromatin and ND10 are cell-cycle regulated and phosphorylation-dependent alternate nuclear sites of the transcription repressor Daxx and SWI/SNF protein ATRX. J. Cell Sci. *117*, 3807–3820. https://doi.org/10.1242/jcs.01230.
52. Ishov, A.M., Sotnikov, A.G., Negorev, D., Vladimirova, O.V., Neff, N., Kamitani, T., Yeh, E.T., Strauss, J.F., 3rd, and Maul, G.G. (1999). PML is critical for ND10 formation and recruits the PML-interacting protein daxx to this nuclear structure when modified by SUMO-1. J. Cell Biol. *147*, 221–234. https://doi.org/10.1083/jcb.147.2.221.
53. Rajagopal, S.K., Ma, Q., Obler, D., Shen, J., Manichaikul, A., Tomita-Mitchell, A., Boardman, K., Briggs, C., Garg, V., Srivastava, D., et al. (2007). Spectrum of heart disease associated with murine and human GATA4 mutation. J. Mol. Cell. Cardiol. *43*, 677–685. https://doi.org/10.1016/j.yjmcc.2007.06.004.
54. Tsuzuki, S., Towatari, M., Saito, H., and Enver, T. (2000). Potentiation of GATA-2 activity through interactions with the promyelocytic leukemia protein (PML) and the t(15;17)-generated PML-retinoic acid receptor alpha oncoprotein. Mol. Cell Biol. *20*, 6276–6286. https://doi.org/10.1128/mcb.20.17.6276-6286.2000.
55. Baumann, C., Schmidtmann, A., Muegge, K., and De La Fuente, R. (2008). Association of ATRX with pericentric heterochromatin and the Y chromosome of neonatal mouse spermatogonia. BMC Mol. Biol. *9*, 29. https://doi.org/10.1186/1471-2199-9-29.
56. McDowell, T.L., Gibbons, R.J., Sutherland, H., O'Rourke, D.M., Bickmore, W.A., Pombo, A., Turley, H., Gatter, K., Picketts, D.J., Buckle, V.J., et al. (1999). Localization of a putative transcriptional regulator (ATRX) at pericentromeric heterochromatin and the short arms of acrocentric chromosomes. Proc. Natl. Acad. Sci. USA *96*, 13983–13988. https://doi.org/10.1073/pnas.96.24.13983.
57. Law, M.J., Lower, K.M., Voon, H.P.J., Hughes, J.R., Garrick, D., Viprakasit, V., Mitson, M., De Gobbi, M., Marra, M., Morris, A., et al. (2010). ATR-X syndrome protein targets tandem repeats and influences allele-specific expression in a size-dependent manner. Cell *143*, 367–378. https://doi.org/10.1016/j.cell.2010.09.023.
58. Zlotorynski, E., Rahat, A., Skaug, J., Ben-Porat, N., Ozeri, E., Hershberg, R., Levi, A., Scherer, S.W., Margalit, H., and Kerem, B. (2003). Molecular basis for expression of common and rare fragile sites. Mol. Cell Biol. *23*, 7143–7151. https://doi.org/10.1128/mcb.23.20.7143-7151.2003.
59. Solomon, L.A., Russell, B.A., Watson, L.A., Beier, F., and Bérubé, N.G. (2013). Targeted loss of the ATR-X syndrome protein in the limb mesenchyme of mice causes brachydactyly. Hum. Mol. Genet. *22*, 5015–5025. https://doi.org/10.1093/hmg/ddt351.
60. Pardue, M.L., and Gall, J.G. (1970). Chromosomal localization of mouse satellite DNA. Science *168*, 1356–1358. https://doi.org/10.1126/science.168.3937.1356.
61. Drouin, R., Lemieux, N., and Richer, C.L. (1991). Chromosome condensation from prophase to late metaphase: relationship to chromosome bands and their replication time. Cytogenet. Cell Genet. *57*, 91–99. https://doi.org/10.1159/000133121.
62. Luciani, J.J., Depetris, D., Missirian, C., Mignon-Ravix, C., Metzler-Guillemain, C., Megarbane, A., Moncla, A., and Mattei, M.G. (2005). Subcellular distribution of HP1 proteins is altered in ICF syndrome. Eur. J. Hum. Genet. *13*, 41–51. https://doi.org/10.1038/sj.ejhg.5201293.
63. Ehrlich, M., Jackson, K., and Weemaes, C. (2006). Immunodeficiency, centromeric region instability, facial anomalies syndrome (ICF). Orphanet J. Rare Dis. *1*, 2. https://doi.org/10.1186/1750-1172-1-2.
64. Xu, G.L., Bestor, T.H., Bourc'his, D., Hsieh, C.L., Tommerup, N., Bugge, M., Hulten, M., Qu, X., Russo, J.J., and Viegas-Péquignot, E. (1999). Chromosome instability and immunodeficiency syndrome caused by mutations in a DNA methyltransferase gene. Nature *402*, 187–191. https://doi.org/10.1038/46052.
65. Berkovich, E., Monnat, R.J., Jr., and Kastan, M.B. (2007). Roles of ATM and NBS1 in chromatin structure modulation and DNA double-strand break repair. Nat. Cell Biol. *9*, 683–690. https://doi.org/10.1038/ncb1599.
66. Kruhlak, M.J., Celeste, A., Dellaire, G., Fernandez-Capetillo, O., Müller, W.G., McNally, J.G., Bazett-Jones, D.P., and Nussenzweig, A. (2006). Changes in chromatin structure and mobility in living cells at sites of DNA double-strand breaks. J. Cell Biol. *172*, 823–834. https://doi.org/10.1083/jcb.200510015.
67. Ziv, Y., Bielopolski, D., Galanty, Y., Lukas, C., Taya, Y., Schultz, D.C., Lukas, J., Bekker-Jensen, S., Bartek, J., and Shiloh, Y. (2006). Chromatin relaxation in response to DNA double-strand breaks is modulated by a novel ATM- and KAP-1 dependent pathway.

Nat. Cell Biol. *8*, 870–876. https://doi.org/10.1038/ncb1446.

68. Lécureuil, C., Fontaine, I., Crepieux, P., and Guillou, F. (2002). Sertoli and granulosa cell-specific Cre recombinase activity in transgenic mice. Genesis *33*, 114–118. https://doi.org/10.1002/gene.10100.
69. Bérubé, N.G., Mangelsdorf, M., Jagla, M., Vanderluit, J., Garrick, D., Gibbons, R.J., Higgs, D.R., Slack, R.S., and Picketts, D.J. (2005). The chromatin-remodeling protein ATRX is critical for neuronal survival during corticogenesis. J. Clin. Invest. *115*, 258–267. https://doi.org/10.1172/jci22329.
70. Barrionuevo, F., Bagheri-Fam, S., Klattig, J., Kist, R., Taketo, M.M., Englert, C., and Scherer, G. (2006). Homozygous inactivation of Sox9 causes complete XY sex reversal in mice. Biol. Reprod. *74*, 195–201. https://doi.org/10.1095/biolreprod.105.045930.
71. Garrick, D., Sharpe, J.A., Arkell, R., Dobbie, L., Smith, A.J.H., Wood, W.G., Higgs, D.R., and Gibbons, R.J. (2006). Loss of Atrx affects trophoblast development and the pattern of X-inactivation in extraembryonic tissues. PLoS Genet. *2*, e58. https://doi.org/10.1371/journal.pgen.0020058.

STAR★METHODS

KEY RESOURCES TABLE

REAGENT or RESOURCE	SOURCE	IDENTIFIER
Antibodies		
Rabbit polyclonal anti-ATRX	Santa Cruz	Cat#sc-15408; Clone: ID H-300; RRID:AB_2061023
Goat polyclonal anti-ATRX	Santa Cruz	Cat#sc-10078; Clone ID: D-19; RRID:AB_634205
Rabbit monoclonal anti-CENP-A	Cell Signaling	Cat#2048; Clone ID: C51A7; RRID:AB_1147629
Rabbit polyclonal anti-TERF1	Alpha Diagnostic	Cat#TRF12-A; RRID:AB_1623614
Rabbit polyclonal anti-DAXX	Santa Cruz	Cat#sc-7152; Clone ID: M-112; RRID:AB_2088784
Rabbit polyclonal anti-FOG-2	Santa Cruz	Cat#sc-10755; Clone ID: M-247; RRID:AB_2218978
Mouse monoclonal anti-GATA4	Santa Cruz	Cat#sc-25310; Clone ID: G-4; RRID:AB_627667
Rabbit polyclonal anti-GATA4	Santa Cruz	Cat#sc-9053; Clone ID H-112; RRID:AB_2247396
Goat polyclonal anti-HP1α	Abcam	Cat#ab77256; RRID:AB_1523784
Rabbit polyclonal anti-PH3 (Ser10)	Sigma-Aldrich	Cat#06–570; RRID:AB_310177
Rabbit polyclonal anti-PML	Santa Cruz	Cat#sc-5621; Clone ID: H-238; RRID:AB_2166848
Rabbit monoclonal anti-γ-H2AX (Ser139)	Cell Signaling	Cat#9718, Clone ID: 20E3; RRID:AB_2118009
Rabbit polyclonal anti-53BP1	Abcam	Cat#ab21083; RRID:AB_722496
Donkey anti-Rabbit IgG (H + L), Alexa Fluor™ 488	Thermo Scientific	Cat#A-21206; RRID:AB_2535792
Goat anti-Mouse IgG (H + L), Alexa Fluor™ 594	Thermo Scientific	Cat#A-11032; RRID:AB_10078167
Donkey anti-Goat IgG (H + L), Alexa Fluor™ 594	Thermo Scientific	Cat#A-11058; RRID:AB_2313737
Biological samples		
Mouse fetal testes	This paper	N/A
Chemicals, peptides, and recombinant proteins		
Antigen Citrate-based unmasking solution	Vector laboratories	H-3300
Critical commercial assays		
NucleoBond Xtra BAC kit	Macherey-Nagel	REF 740436.2
Experimental models: Organisms/strains		
Mouse: *AMH-Cre/+*: *Plekha5*$^{Tg(AMH\text{-}cre)1Flor}$	Florian Guillou[68]	MGI:2450300
Mouse: *Atrx*$^{flox/flox}$: *Atrx*^{tm1Rjg}	Doug Higgs[69]	MGI:3528480
Oligonucleotides		
Primer used for Sanger sequencing to confirm the sequence of BAC DNA (Yp) F1: TGACATTGTAGGACTATATTGC	This paper	N/A
Primer used for Sanger sequencing to confirm the sequence of BAC DNA (Yq) R1: ATCTGCCGTTTCGATCCTCC	This paper	N/A
Primer used for Sanger sequencing to confirm the sequence of BAC DNA (Yp) F2: CACTCAGAGTTGAGACTTTGAAGCA	This paper	N/A
Primer used for Sanger sequencing to confirm the sequence of BAC DNA (Yp) R2: TGGCTTAGCAACAGACAAGTGC	This paper	N/A
Primer used for Sanger sequencing to confirm the sequence of the Yq probe F3: ATACTACTCTAGAATACTGCATGC	This paper	N/A

(*Continued on next page*)

Continued

REAGENT or RESOURCE	SOURCE	IDENTIFIER
Primer used for Sanger sequencing to confirm the sequence of the Yq probe R3: TGTAGTCATCAAATGGTTTCCAAG	This paper	N/A
Recombinant DNA		
Yp probe for FISH: BAC clone B6Ng01-016L17; contains 73.6 kb of the short arm of the Y chromosome	Dr. Yusuke Miyanari[29]	B6Ng01-016L17
Yq probe for FISH: 1.8 kb dispersed repeats	Dr. Paul Kalitsis[41,42]	N/A
Software and algorithms		
Fiji software	Fiji software[32] website: fiji.sc	N/A
GraphPad Prism v8.1	GraphPad by Dotmatics website: www.graphpad.com	N/A

RESOURCE AVAILABILITY

Lead contact

Further information and requests for resources and reagents should be directed to and will be fulfilled by the lead contact, Vincent Harley (vincent.harley@hudson.org.au).

Materials availability

This study did not generate new unique reagents.

Data and code availability

- All data reported in this paper will be shared by the lead contact upon request.
- This paper does not report original code.
- Any additional information required to reanalyze the data reported in this paper is available from the lead contact upon request.

EXPERIMENTAL MODEL AND STUDY PARTICIPANT DETAILS

Mice and ethics

All animal experimentation was approved and performed according to procedures determined by the Monash Medical Centre Animal Ethics Committee. *Atrx*$^{flox/flox}$[69] and *AMH-Cre/+* mice[68] were obtained from Doug Higgs and Florian Guillou, respectively. 2- to 6-month-old *Atrx*$^{flox/flox}$ female mice (C57BL/6) were crossed with 2- to 6-month-old *AMH-Cre/+* male mice (C57BL/6) to generate *AMH-Cre/+*; *Atrx*$^{flox/Y}$ (Sc*Atrx*KO) male embryos. *Atrx*$^{flox/Y}$ male embryos were used as controls. For embryonic time points, noon of the day after mating was considered E0.5. Dissection of whole embryos was performed at E16.5 and E17.5. For genotyping, genomic DNA was isolated from tail tissue and subjected to genotyping using a previously published protocol.[70,71]

Tissue processing and paraffin sectioning

Mouse embryos were collected at day E16.5 and E17.5, washed with 1X PBS and fixed with 4% paraformaldehyde (PFA). Fixed embryos were sent to the Histopathology platform at the Hudson Institute of Medical Research for tissue processing and paraffin embedding. Sagittal sections of the embryos were generated with a microtome at 4 μm thickness.

METHOD DETAILS

Immunofluorescence

Paraffin testis sections of Sc*Atrx*KO and control *Atrx*$^{flox/Y}$ male mice were sent to the Histopathology platform at the Hudson Institute of Medical Research for dewaxing. The slides were heated at 60° degrees and dipped in xylene to remove the paraffin. Then, the slides were placed in 100% EtOH 3 times for 3 minutes each followed by dipping in distilled water (dH2O) for 5 minutes. Heat-induced epitope retrieval was done using a pressure cooker containing 15 mL of Antigen Citrate-based unmasking solution (Vector laboratories; H-3300), diluted in 1.6 L of dH2O. For immunofluorescence, sections were blocked in blocking solution (1X PBS with 0.1% Tween20 and 5% donkey serum) for 1 hour at room temperature. Then, the sections were incubated with diluted primary antibodies at 4°C overnight. On the next day, the slides were washed

with 1X PBS 3 times for 5 minutes each and incubated with secondary antibodies for 1 hour. Table S1 contains a list of the primary and secondary antibodies used in this study.

To reduce autofluorescence, Sudan Black solution (0.1% in 70% EtOH) was applied to the slides which were incubated at room temperature for 8 minutes. After washing with 1X PBS, the slides were counterstained with DAPI (1:5000) for 5 minutes at room temperature, and then washed in 1X PBS. Finally, the slides were mounted using fluorescent mounting medium (Dako). Imaging was performed using confocal microscopes (Olympus FV1200 and Nikon C1, Monash Imaging).

Preparation of BAC DNA

The BAC clone B6Ng01-016L17[29] which contains 73.6 kb of the short arm of the Y chromosome was provided by Dr. Yusuke Miyanari from Kanazawa University. For preparation of the BAC DNA, the BAC strain was first cultured on a LB agar plate containing 25 μg/mL of chloramphenicol and incubated at 37°C overnight. Then, a single colony was cultured in 2 mL of LB Broth media with 25 μg/mL of chloramphenicol and incubated at 37°C for 8 hours. The 2 mL were added to 500 mL of LB Broth media with 25 μg/mL of chloramphenicol and incubated overnight at 37°C. The culture medium was then centrifuged at 4,000 rpm for 10 minutes at room temperature. The BAC DNA was purified using the NucleoBond Xtra BAC kit (Macherey-Nagel 740436.2) following the manufacturer's protocol. Finally, BAC DNA was resuspended in 700 μL of sterile H_2O and incubated overnight at 4°C to dissolve completely. The sequence of the BAC DNA was confirmed by Sanger sequencing using the primers listed in Table S2.

Immuno-FISH

Dewaxed sections of Sc*Atrx*KO and control $Atrx^{flox/Y}$ mice were first stained with a GATA4 antibody using the immunofluorescence protocol described above. Afterwards, FISH was performed starting with the dehydration of the slides in an ethanol series of 75%, 80% and 100%, and then air-dried. To denature, slides were placed in 2X SSC/Formamide at 80°C for 5 minutes. After drying the slides, they were treated with a cold ethanol series of 75%, 80%, and 100%, and then dried again. The Yp and Yq DNA probes (Table S3) were heated at 95°C for 5 mins and immediately placed on ice.

The probe was added to the slide and a coverslip was placed on top, sealing the edges with glue. The slides were then placed in an opaque and humidified chamber and were incubated at 37°C overnight. The next day, the slides were washed 3 times with 2X SSC for 5 minutes each, followed by 2 times with 0.5X SSC for 5 minutes each, at room temperature. TNB block was added to each slide and incubated for one hour at 37°C. Next, the slides were incubated with AV488 (1/400) for one hour at 37°C. The slides were then washed 3 times with 4X SSC +0.1% Tween-20 for 5 minutes each time. They were quickly rinsed in PBS solution, fixed in 4% PFA for 7 minutes and air-dried. Finally, for nuclei detection, DAPI was applied, and the slides were kept in the dark at 4°C. Imaging was performed using confocal microscopes (Olympus FV1200 and Nikon C1, Monash Imaging).

QUANTIFICATION AND STATISTICAL ANALYSIS

Quantification of cell numbers

To determine the average percentage of Sertoli cells that were positive for GATA4, PH3, γ-H2AX and PML, the total number of Sertoli cells and marker-positive cells was manually counted, using cell count tool of Fiji software.[32] More than 800 Sertoli cells were analysed in each testis (control $n = 2$; Sc*Atrx*KO = 3). A second blind observer also performed the quantification, obtaining similar results. Graphs and statistical analysis were done using GraphPad Prism v8.1 (www.graphpad.com).

Measurement of GATA4 foci diameter

A total of 3 control and 4 Sc*Atrx*KO testes were analysed, using Fiji software.[32] More than 100 GATA4 foci and GATA4-PML NBs were measured in each testis. To determine their size a threshold was applied as the GATA4 foci/GATA4-PML NBs presented the most intense signal in the image. Then, specific parameters were set based on the scale bar of each image, and the program did an automatic measurement of the area and perimeter of the foci. All images were analysed under the same parameters. Finally, GraphPad Prism v8.1 software (www.graphpad.com) was used to obtain graphs and perform the statistical analysis.

Statistical analysis

All statistical analysis was conducted with GraphPad Prism v8.1 (www.graphpad.com). Statistical significance was determined by two-tailed t-test or one-way ANOVA analyses. The appropriate tests and the number of replications are stated in the figure legends. Values are the mean ± SEM. A p value <0.05 was utilized as the cut-off for statistical significance. All statistics are $*p < 0.05$, $**p < 0.01$, $***p < 0.001$, $****p < 0.0001$.